

Resting-State Functional Connectivity and stimulation-induced neural activity in the cortex and sub-cortical structures of Rat Brain

F. Zhao¹, T. Zhao¹, L. Zhou¹, Q. Wu¹, Z. Yang¹, and X. Hu¹

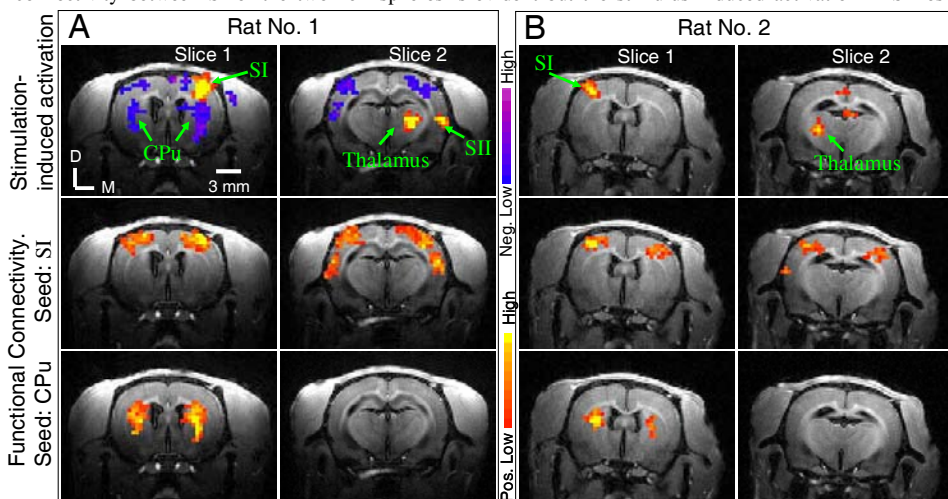
¹Coulter Department of Biomedical Engineering, Emory / Georgia Tech, Atlanta, Georgia, United States

INTRODUCTION Functional connectivity in the brain can be investigated by using correlated low-frequency fluctuations in the resting-state MRI signal (1). Recent studies have shown that such resting-state fMRI can be used as an index to evaluate pathological conditions such as Alzheimer's disease (2) and drug effects (3, 4). To date, most resting-state fMRI studies have been performed on human subjects with few on animals – probably due to the use of anesthesia in animal models (5). Even though resting-state connectivity was detected in the α -chloralose anesthetized rat (6, 7), the relationship between resting-state functional connectivity and stimulation-induced activation has not been fully studied in animal models. Furthermore, functional connectivity involving subcortical structures, as reported in human subjects (8), has not been detected in animals. With these observations in mind, the present study further investigates the rest-state connectivity in a rat model. More specifically, because resting-state is influenced by anesthesia and domitor has been used for anesthesia in rat fMRI (9), we performed fMRI with forepaw electrical stimulation and resting-state fMRI in domitor-anesthetized rat at 9.4 T to probe this phenomenon.

METHOD Five rats (250–350 g) were anesthetized initially with 5% isoflurane in O₂:N₂ (3:7), which was reduced to 2% for maintenance. A pair of needle electrodes was inserted into a single forepaw for electrical stimulation. A bolus of 0.05 mg/kg domitor was injected subcutaneously, and isoflurane was disconnected 10 minutes afterwards. A mixture of O₂:N₂ (3:7) was delivered to the nosecone for spontaneous respiration. Continuous subcutaneous infusion of domitor (0.1 mg/kg/hour) was started 15 minutes after the bolus injection. Rectal temperature was maintained at ~37°C by a feedback-controlled, water-circulated heating pad and blood oxygen saturation was monitored by non-invasive oxygen saturation monitor during the preparation and fMRI experiments. MR measurements were performed on a 9.4T/20cm system (Bruker) with a 2-cm diameter actively-decoupled surface coil as a receiver and a 72 mm actively-decoupled volume coil as a transmitter. Eight consecutive axial slices were imaged with TE=15 ms, thickness = 1 mm, matrix size = 64×64 and FOV = 3×3 cm², using single-shot GE EPI. For stimulation-induced fMRI study, each fMRI run consisted of 10 – 10 – 20 image acquisitions (boldface represents stimulation on) with TR = 2 s. Electrical stimulation pulses had a 0.3 ms width, frequencies ranging from 1 to 18 Hz and currents ranging from 1 to 8 mA. Stimulation-induced fMRI study lasted ~3 hours. Subsequently, a total of 300 images (10 minutes) with exact the same parameters were acquired without stimulation (i.e., resting-state). For data analysis of stimulation-induced fMRI, statistical *t* value maps were calculated by comparing the images acquired during the control and stimulation periods on a pixel-by-pixel basis and thresholded with *t*-value > 3 and cluster size > 4 pixels (*p*<0.01). For data analysis of resting-state fMRI, a low-pass filter was used to eliminate the high frequency component (>0.08 Hz). Based on the stimulation-induced fMRI maps, an ROI (2×2 pixels) was selected in the primary somatosensory cortex (SI), the Caudate Putamen (CPu) and the thalamus separately and the average time courses from these ROIs were used as references to calculate the cross-correlation coefficient (CCC) for all pixels. A threshold of CCC>0.3 and cluster size >4 was used to functional connectivity maps.

RESULTS Figs. A and B show the results from two different rats. The 1st row shows the single-forepaw-stimulation-induced activation maps in the SI (Slice 1), the secondary somatosensory cortex (SII) and the thalamus (Slice 2). Interestingly, negative BOLD responses were detected in the caudate putamen (CPu) and some bilateral cortical regions when strong stimulus was used (e.g., Fig. A). The second row illustrates the functional connectivity with a seed in SI. They exhibit significant activation in extended cortical regions of both hemispheres. The third row presents functional connectivity maps obtained using CPu ROI as a seed. These maps exhibit significant connectivity of the CPu in the two hemispheres. When choosing thalamus ROI as a seed, no connectivity can be detected (data not shown). Consistent results were obtained in all five rats.

DISCUSSION In consistency with human studies (1), our results show that there is a correlation of low-frequency fluctuations in resting-state fMRI signal in domitor-anesthetized rat. Bilateral correlation exists in extended cortical area and CPu. The resting-state maps are symmetric in the two hemispheres, indicating strong inter-hemispheric connection. There is no connectivity between cortex and CPu during the resting-state. We have also tested the relationship between the resting-state connectivity and stimulation-induced activation. In the cortex, anatomical correspondence between stimulation-induced activation and resting-state maps is limited. The connectivity between SI of the two hemispheres is evident but the stimulus induced activation in SI resides mainly unilaterally. This suggests that the functional connectivity in the rest state can identify the entire relevant network while a specific task (e.g., single forepaw somatosensory) can only activate the corresponding region. In CPu, negative BOLD response on both sides can be robustly detected when using high stimulation on single forepaw (see Fig. A) and a strong resting-state connectivity are detected, possibly indicating the functional correlation between the two sides of CPu. For thalamocortical connection, both thalamus and SI are activated during forepaw stimulation while no connection is detected during resting state, indicating that thalamus only takes charge of afferent nerves to somatosensory cortex, not efferent nerves. In summary, the resting-state maps observed in this study paves the way for future exploration of resting-state fMRI mechanism and extending the application of such phenomenon to neuroscience research and drug development.



connectivity in the rest state can identify the entire relevant network while a specific task (e.g., single forepaw somatosensory) can only activate the corresponding region. In CPu, negative BOLD response on both sides can be robustly detected when using high stimulation on single forepaw (see Fig. A) and a strong resting-state connectivity are detected, possibly indicating the functional correlation between the two sides of CPu. For thalamocortical connection, both thalamus and SI are activated during forepaw stimulation while no connection is detected during resting state, indicating that thalamus only takes charge of afferent nerves to somatosensory cortex, not efferent nerves. In summary, the resting-state maps observed in this study paves the way for future exploration of resting-state fMRI mechanism and extending the application of such phenomenon to neuroscience research and drug development.

Fig. Stimulation-induced activation and resting-state

connectivity with Domitor for anesthesia in two rats. The 1st row shows electrical forepaw stimulation-induced activation maps in the slices of primary somatosensory cortex (SI, Slice 1) and of secondary somatosensory cortex (SII) and thalamus (Slice 2). The 2nd row presents resting-state connectivity with a seed in SI. The 3rd row is resting-state connectivity with a seed in CPu. All activation maps are overlaid on the T1-weighted anatomical images. D: dorsal; M: Medial; SI & SII: primary & secondary somatosensory cortices; CPu: Caudate Putamen. Color bars are *t*-values (3-12) for first row and CCC (0.3-0.6) for 2nd and 3rd rows.

REFERENCE 1. Biswal B, et al., *Mag Reson Med* 1995;34:537-541. 2. Li S-J, et al., *Radiology* 2002;225:253-259. 3. Li S-J, et al., *Mag Reson Med* 2000; 43:45-51. 4. Anand A, et al., *Neuropsychopharmacology* 2005;30:1334-1344. 5. Peltier S, et al., *NeuroReport* 2005;16:285-288. 6. Lu H, et al., *ISMRM* 2006;532. 7. Williams KA, et al., *ISMRM* 2006;2119. 8. Stein T, et al., *AJNR* 2000;21:1397-1401. 9. Weber R, et al., *Neuroimag* 2006;29:1303-1310. ((Supported by NIH EB002009 and Georgia Research Alliance)